© 2016. Published by The Company of Biologists Ltd | Journal of Experimental Biology (2016) 219, 1432-1436 doi:10.1242/jeb.132084

METHODS & TECHNIQUES

Quantification of sarcomere length distribution in whole muscle frozen sections

Shawn M. O'Connor[1,2], Elton J. Cheng[1], Kevin W. Young[1,3], Samuel R. Ward[1,2,3,4] and Richard L. Lieber[1,2,3,5,*]

ABSTRACT

Laser diffraction (LD) is a valuable tool for measuring sarcomere length (L_s), a major determinant of muscle function. However, this method relies on few measurements per sample that are often extrapolated to whole muscle properties. Currently it is not possible to measure L_s throughout an entire muscle and determine how L_s varies at this scale. To address this issue, we developed an actuated LD scanner for sampling large numbers of sarcomeres in thick whole muscle longitudinal sections. Sections of high optical quality and fixation were produced from tibialis anterior and extensor digitorum longus muscles of Sprague–Dawley rats (N=6). Scans produced two-dimensional L_s maps, capturing >85% of the muscle area per section. Individual L_s measures generated by automatic LD and bright-field microscopy showed excellent agreement over a large L_s range (ICC>0.93). Two-dimensional maps also revealed prominent regional L_s variations across muscles.

KEY WORDS: Laser diffraction, Muscle architecture, Sarcomere length

INTRODUCTION

Laser diffraction (LD) is used to measure sarcomere length (L_s) in muscle. L_s is an important physiological parameter because it directly determines muscle fiber active force production (Gordon et al., 1966) and is therefore closely coupled with muscle function (Winters et al., 2011). Muscle diffraction is possible because sarcomere structure consists of light and dark bands due to actin and myosin filament arrays. This optical characteristic causes muscle to act as a phase grating to incident laser light and allows diffraction grating spacing (equivalent to L_s) to be calculated (Yeh et al., 1980).

Typically, individual L_s measurements are obtained from small illuminated regions within a muscle sample and these are extrapolated to whole muscle properties. Average L_s of whole muscle is typically estimated *ex vivo* by dissecting a limited number of fibers at distributed locations along the muscle, measuring L_s at points along individual fibers and then averaging results (Felder et al., 2005). Although LD methods sample up to thousands of sarcomeres, depending on beam diameter, this sample size is many orders of magnitude smaller than the total number of sarcomeres contained in whole muscle. By contrast, light microscopy usually samples only hundreds of sarcomeres, depending on magnification (Huxley and Peachey, 1961; see table 1 in Young et al., 2014).

[1]Department of Bioengineering, University of California San Diego, La Jolla, CA 92093, USA. [2]Department of Orthopaedic Surgery, University of California San Diego, La Jolla, CA 92093, USA. [3]Research Service, Veteran's Administration San Diego Healthcare System, San Diego, CA 92161, USA. [4]Department of Radiology, University of California San Diego, La Jolla, CA 92093, USA. [5]Rehabilitation Institute of Chicago, Chicago, IL 60611, USA.

*Author for correspondence (rlieber@ric.org)

Received 15 September 2015; Accepted 2 March 2016

Whereas to a first approximation, a muscle's active tension-generating properties can be explained based on L_s (Winters et al., 2011), little is known about the degree to which L_s varies across a muscle and how this variation influences function. It is also unclear whether L_s variation is related to other muscle properties, such as fiber type distribution, boundary condition asymmetry or regional stress concentrations. Additionally, there are certain pathological conditions where the L_s versus force relationship appears to be disrupted and where the correlation between serial sarcomere number and muscle excursion is lost (e.g. Takahashi et al., 2012). In these cases, it would be important to document L_s variability throughout the entire muscle. However, creating such 'meso-scale' L_s distributions is currently impossible. To address this problem, we developed an automated device to scan a large muscle cross-sectional area with a laser device to create diffraction patterns across sections and then validated the method by comparing the L_s values with those obtained by bright-field (BF) microscopy.

MATERIALS AND METHODS

Hardware design

A motorized stage was incorporated into a standard LD system (Lieber et al., 1990) such that slide-mounted longitudinal muscle sections could be translated in the horizontal plane relative to the laser path (Fig. 1A). A vertically mounted 635 µm wavelength laser transilluminated sections from below (Lablaser, Coherent). Beam width was reduced using a 800 µm precision pinhole (Edmund Optics) placed directly over the laser face and laser power was controlled by analog input signal to the laser power supply. The resultant diffraction pattern was measured by a 1024 element linear photodiode array (L-series CMOS, Excelitas Technologies), centered directly above the laser path. Sensor resolution was a non-linear function of L_s with a minimum 0.03 µm resolution at the highest expected L_s value of 4 µm.

The actuation system for translating slide-mounted muscle sections (Fig. 1A) was a linear servo motor system (MS-2052, ASI). The system controlled the x–y location (SI-INV-UNI, ASI) with 0.1 µm resolution and <0.7 µm repeatability. The motors were controlled directly using a microcontroller-based stage controller unit (MS2, ASI) with internal position feedback control. The controller unit communicated with a custom MatLab script to receive position commands and send motor state parameters via an RS-232 serial communication protocol.

Software and user interface design

Custom MatLab software controlled the motorized stage to systematically scan the laser beam across the section, record diffraction patterns and calculate L_s. Slides were mounted to the stage insert such that fibers were parallel to the photodiode array and anatomical orientation was consistent across slides. A MatLab-based GUI then allowed selection of bounding points that defined the scanning region. Points were selected by translating the slide

Journal of Experimental Biology

Journal of Experimental Biology (2016) 219, 1432-1436 doi:10.1242/jeb.132084

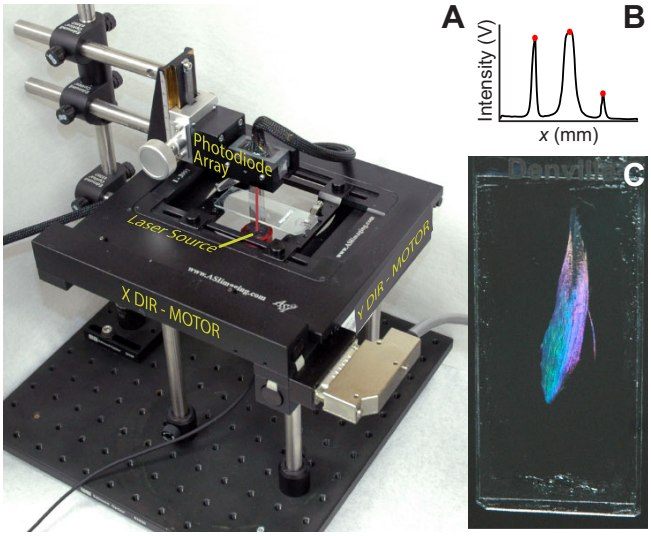

Fig. 1. Laser diffraction (LD) device scans longitudinal muscle sections. (A) Motorized laser diffraction device. Two motors move a stage holding a slide-mounted muscle section through a laser beam path (red line). A photodiode array measures the diffraction pattern at each sample location. (B) Example diffraction signal (black line) of intensity (volts) as a function of position along the photodiode array. Custom software automatically identifies peak locations (red dots) and calculates L_s. (C) Example embedded sagittal plane longitudinal section of a rat TA muscle transilluminated with visible light in which white light diffraction is apparent through a majority of the sample as a rainbow pattern.

stage via a joystick located on the stage controller and were visualized by laser beam scattering on the slide face. The user was also prompted to define the proximal and distal muscle fiber landmark locations, which were stored for subsequent serial section alignment.

Diffraction patterns were sampled with 400 µm spacing within the scanning region at approximately 50 points per minute. The diffraction pattern from the photodiode array was sampled at 30.5 Hz (NI USB-6251, National Instruments Corporation) and five sequential patterns were obtained per point, averaged and smoothed (Garcia, 2010) (Fig. 1B). This acquisition rate enabled sarcomere mapping of about 8 mm^2 min^{-1}. The diffraction peak locations were then used to calculate L_s based on the grating equation (Lieber et al., 1984). An additional diffraction pattern was sampled with the laser at half power, automatically set by an analog input to the laser power supply (NI USB-6251). Tissue transparency was quantified based on the zeroth order peak voltage at low laser power. Peak voltage values were normalized between 0 and 1 to represent the range of voltage values for each slide, where a value of 1 represents the most transparent measurement locations. The higher power setting ensured that diffraction peaks were sufficiently large whereas the lower power supply prevented the zeroth order peak voltage from saturating.

Muscle harvesting and sample preparation

All procedures were approved by the University of California Institutional Animal Care and Use Committee. Tibialis anterior (TA; N=6) and extensor digitorum longus (EDL; N=6) muscles were obtained from male Sprague–Dawley rats between the ages of 10 and 13 weeks. Power analysis indicated this sample size was appropriate to detect a 0.08 µm L_s difference. Half the muscles were preserved using transcardial perfusion fixation, as previously described (Mathieu-Costello, 1987). The lower limbs were fixed with hip and knee joints at 90 deg and ankle joints held at resting length (0 deg dorsiflexion). The second half of muscles were fixed after animals were euthanized with carbon dioxide. Whole lower limbs were dissected and positioned with knee joints at 90 deg and ankle joints held at a stretched length (fully plantarflexed) and immersed in fixative for 2–3 days. After fixation, muscle samples were dissected, rinsed in 1× phosphate-buffered saline (PBS), blotted dry and weighed.

We used a combination of sucrose cryo-protection and pre-chilling samples prior to snap-freezing to obtain samples with minimal freeze damage. Samples were transferred to 15% and then 30% sucrose solution in 1×PBS, each for 24 h (McNeil and Khakee, 1992). Sucrose solution is a natural cryo-protectant and allowing sucrose solution to displace water in the intercellular spaces prevents ice crystal formation during freezing (Scouten et al., 2006). Muscles were then divided longitudinally into medial and lateral halves, embedded in optimal cutting temperature (OCT) compound, chilled at 4°C for 30 min, snap-frozen in isopentane cooled with liquid nitrogen and transferred to the cryostat chamber. We believe that pre-chilling muscle samples to 4°C reduces crystal and crack formation during snap freezing by speeding transition to the freezing point.

Samples were cryo-sectioned longitudinally at 100 µm thickness through the entire muscle. Cryostat chamber and object temperature were −15°C and −10°C, respectively, to accommodate the higher stiffness of fixed frozen tissue over fresh frozen tissue. Each section was first transferred to a 1×PBS bath to dissolve excess OCT. Sections were then mounted by floating each section onto a microscope slide and draining excess liquid with a pipet and lint-free wipe. This technique ensured that muscle morphology and shape were preserved and consistent from section to section. Slides were stored in a humidification chamber until ready for further processing. They were then coverslipped using aqueous mounting medium (VectaMount AQ, Vector Laboratories), dried for 2–3 days and then sealed (CoverGrip Coverslip Sealant, Biotium). The result of this fixation and sectioning process was an embedded sagittal plane longitudinal section (Fig. 1C).

A limited number of serial sections at 50 and 100 µm thickness were also produced to compare the effect of thickness on diffraction measurements. 20 µm sections were also attempted during initial piloting but these sections often tore during slide deposition and were excluded from further testing. The 50- and 100-µm-thick sections were cut sequentially in the lateral portions of the TA muscles and the sequence was repeated three times.

Analysis

The automatic LD scanner was initially validated by scanning two slide-mounted diffraction gratings (1.67 and 3.33 µm spacing) and quantifying measurement accuracy and precision. To quantify muscle section quality and L_s accuracy, two slides per muscle, one each from the medial and lateral halves, were scanned. The degree to which sections produced viable L_s measurements was used to define quality. The transparency metric first identified scan locations containing tissue based on values below a maximum threshold. Yield was then defined as the percentage of measured L_s values out of the number of identified tissue locations.

Sarcomere length measurements automatically determined by LD were also compared with measurements using BF microscopy to validate system accuracy. For each section, seven measurement points were chosen for comparison that represented the minimum and maximum L_s values as well as the 16.7, 33.3, 50, 66.7 and 83.3 percentile values. Custom software converted x–y locations of the seven points to microscope stage coordinate system using the

Journal of Experimental Biology (2016) 219, 1432-1436 doi:10.1242/jeb.132084

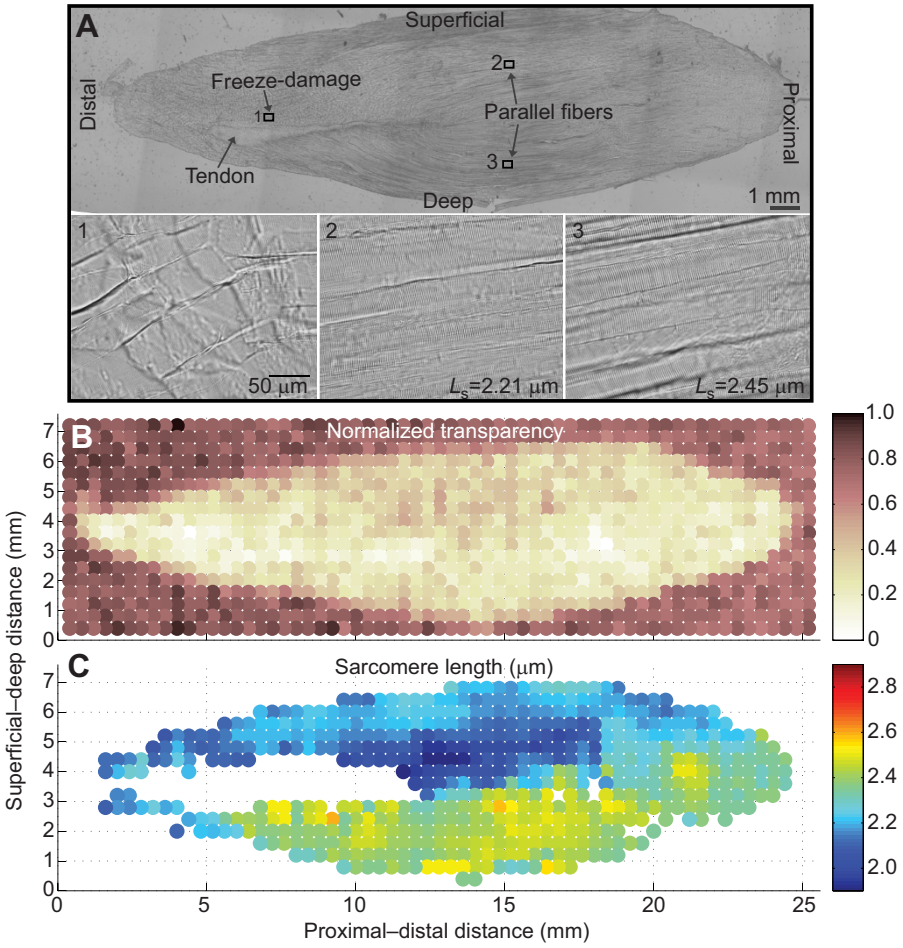

Fig. 2. L_s and transparency mapping in a TA muscle section. (A) Bright-field (BF) microscope image of an example longitudinal TA muscle section at 2.5× containing an internal tendon, well-preserved muscle fibers and a small area with freeze damage. Distal and superficial directions are to the left and up, respectively. Magnified images of three specific areas (labeled 1–3) at 40× are highlighted. (B) Normalized transparency index sampled across an example longitudinal TA section in 400 µm increments. Transparency is highest in non-tissue regions, lowest in regions containing muscle or tendon and therefore transparency enables determination of section size and shape. (C) L_s sampled across a longitudinal TA section in 400 µm increments. L_s was successfully measured in regions that did not contain tendon or freeze damage.

proximal and distal muscle locations as reference points, marked by a small drop of permanent ink placed on the slide. A microscope (Model DM6000, Leica Microsystems) was used to capture BF images of the seven muscle locations using a 40× objective. The BF image area occupied approximately 13% of the area illuminated by the laser and sampled through diffraction. MatLab software analyzed each image and calculated average L_s using fast Fourier transform (FFT) analysis (Weiwad et al., 2000).

For each muscle, we determined the root-mean-square (RMS) error between LD and BF L_s measures as percentages of the BF measurement and then computed TA and EDL group averages. Intraclass correlation coefficients (ICCs) quantified absolute agreement between L_s values produced by the two methods, where ICC>0.8 was defined as excellent agreement. Agreement was visualized using Bland–Altman plots.

Mean and coefficient of variation (CV) of measured L_s were computed from the subset of serial TA slides at 50 and 100 µm. ICCs quantified absolute agreement between mean and CV measures at the two thicknesses. Significance was determined as P<0.05, and data are presented as means±s.d.

RESULTS AND DISCUSSION

The scanner was initially validated by measuring 1000 samples from two diffraction grating slides (1.77 and 3.34 µm fixed spacings). Average measured spacing for the two gratings were 1.768±0.002 and 3.347±0.010 µm (mean±s.d.), respectively, corresponding to −0.1 and 0.2% errors. CV of individual spacing measures were 0.10 and 0.31%, respectively. Sensor resolution and noise, variations in grating spacing and miscalibration are potential sources of these measured errors.

Longitudinal sections of high optical quality and fixation were produced from TA and EDL muscles and scanned to produce two-dimensional L_s maps. BF images revealed optically clear sections with well-preserved muscle fibers (Figs. 2A, 3A). Regions with identifiable freeze damage generally did not produce diffraction patterns with distinct peaks. Laser intensity control was sufficient to produce a transparency measure to identify each section's shape and size (Fig. 2B). Transparency was highest in non-tissue regions and lowest in regions containing internal tendon, which compared well with microscope image features. Sarcomere length was successfully measured in regions that did not contain tendon or freeze damage (Figs. 2C, 3B). On average, 611±151 and 349±65 L_s measurements were produced per muscle section for TA and EDL, respectively whose dimensions were approximately 98 and 56 mm^2. Across all sections, tissue preparation and scanning processes yielded 85.2±13.8% and 88.0±5.3% useable area for TA and EDL muscles, respectively.

Measurement accuracy was validated by comparing a subset of L_s values determined by LD with values measured from the same muscle locations by BF microscopy (Fig. 3C,D). Two slides per muscle and seven points per slide were compared. For TA muscles, average RMS error between LD and BF measures was 1.59±0.65%, as a percentage of BF measures. ICCs quantified absolute agreement between the two methods. The mean ICC value among TA muscles was 0.98±0.01. For EDL muscles, average RMS error was 2.56±1.06% and average ICC value was 0.93±0.06.

Journal of Experimental Biology

Journal of Experimental Biology (2016) 219, 1432-1436 doi:10.1242/jeb.132084

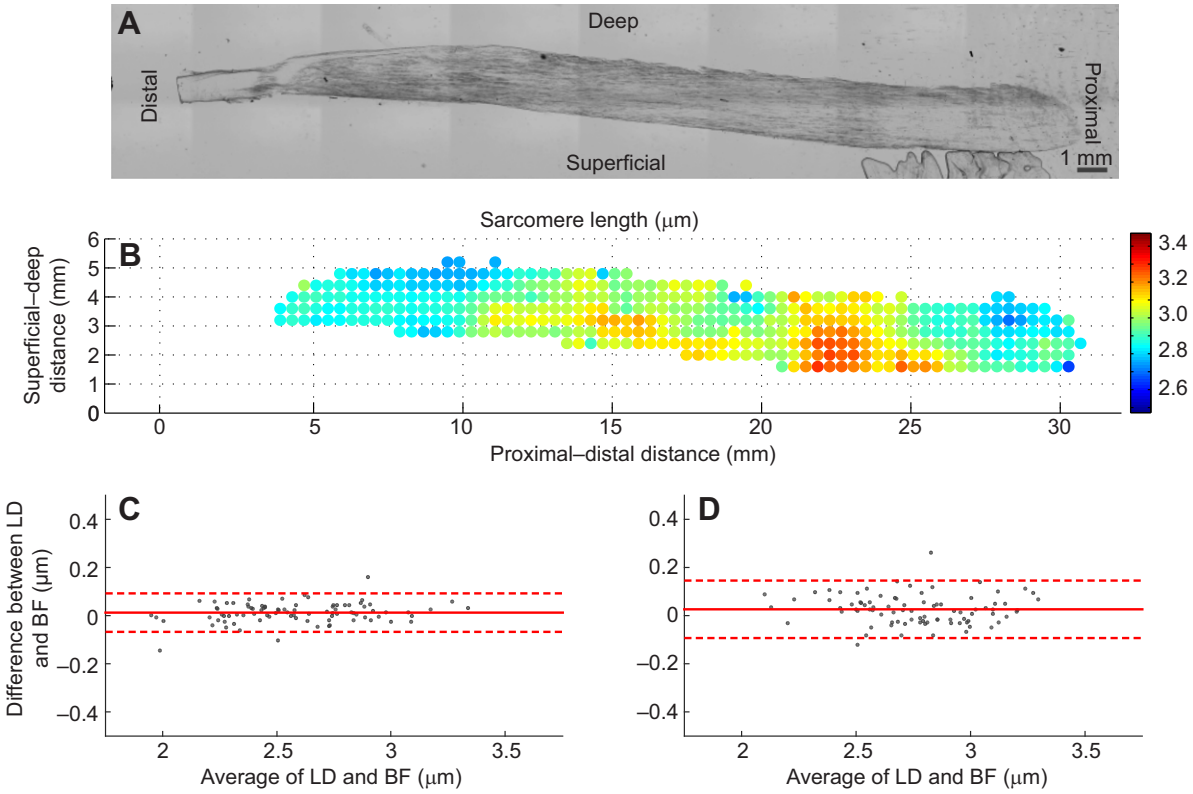

Fig. 3. L_s mapping in EDL muscle section and Bland–Altman comparisons for TA and EDL. (A) BF microscope image of a sample longitudinal EDL muscle section at 2.5×. Distal and superficial directions are to the left and up, respectively. (B) L_s sampled across longitudinal EDL section in 400 μm increments. L_s values at a subset of scan locations were compared with values measured from the same muscle locations using BF microscopy. Bland–Altman plots for TA (C) and EDL (D) muscle. Measurement accuracy for each muscle was validated by comparing a subset of L_s values determined by LD with values measured from the same muscle locations by BF microscopy. Two slides per muscle (N=6) and seven points per slide were compared. Red lines represent the mean difference between measurements and red dashed lines represent the 95% limits of agreement.

The impact of section thickness on diffraction measurements was also determined. Mean and CV of L_s demonstrated excellent agreement between serial 50 and 100 μm TA sections (both ICC>0.99). In terms of spatial resolution, thinner sections increase the likelihood of sampling from single muscle fibers in depth, which typically have fiber diameters of 10–100 μm (Lieber, 2010). However, attempts to produce 20 μm sections were confounded by inconsistent section quality and tissue damage during section manipulation.

This methodology is subject to a number of limitations. First, diffraction patterns were measured using a linear photodiode array, which limits measures to muscles with relatively uniform muscle fiber orientation that must be aligned with the detector. In this system, calculated sarcomere length errors are small (<3%) for misalignments within ±15 deg, which would be easy to detect and diffraction peaks are not measured outside ±20 deg because diffracted laser light misses the photodiode array. Upgrading to a two-dimensional array would allow sampling from muscles with non-uniform pennation angles, but this modification was not necessary for the muscles tested here.

A second source of error is caused by a skew angle between the sectioning plane and the fiber trajectories such that whole fibers

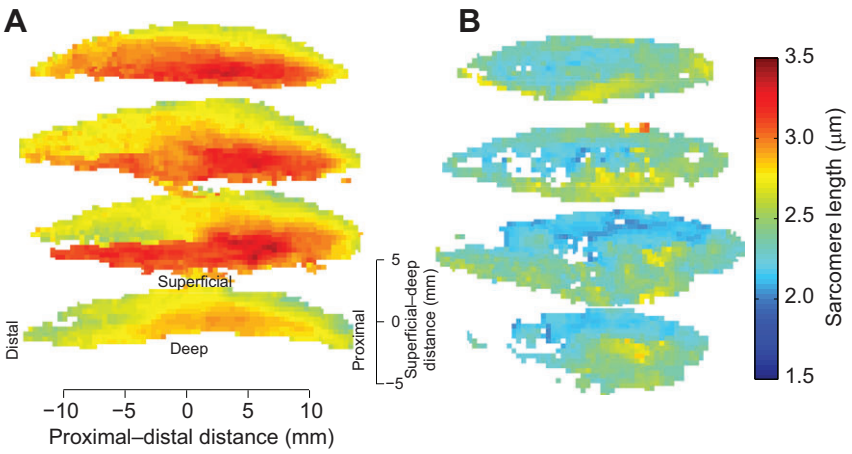

Fig. 4. Two-dimensional L_s maps of four equally spaced sagittal plane sections in resting and stretched TA muscle. High-yield L_s maps were produced throughout the muscle volume. Comparison of multiple TA sections when stretched (A) or resting (B) provides visualization of 3D L_s variation.

Journal of Experimental Biology (2016) 219, 1432-1436 doi:10.1242/jeb.132084

are not captured within a single section, which are only 100 µm thick. Diffraction patterns result from two optical phenomena, grating interference and Bragg interference, the latter of which is sensitive to skew. Average L_s will be accurate and effects of skew will be relatively insignificant if the grating contributions dominate, as is the case for conditions where the laser beam diameter is significantly larger than the fiber diameter (Lieber et al., 1984). Conditions similar to those tested in this experiment showed an average error of <1.5% over a range of incident angles (±15 deg). Light microscopy inspection also generally revealed long, unbroken fiber segments within sections. These effects could be considered if sectioning muscles with complex fiber trajectories, but do not significantly alter the conclusions presented here.

Third, measurement spacing and the number of sarcomeres sampled per measurement are limited by laser beam diameter. At a beam diameter of 800 µm, each L_s measure samples from thousands of sarcomeres. Beam diameter may be scaled based on muscle size or sampling needs by varying the precision pinhole diameter. Use of smaller diameter lasers may require thinner sections to limit Bragg effects (Lieber et al., 1984), although section thickness is practically limited to 50 µm.

Finally, the transparency metric used to quantify percentage yield identified scan locations containing tissue based on a minimum threshold but did not distinguish between tendon, muscle or fascia. Therefore, percentage yield values presented in this study are likely to be underestimates of the true yield of viable L_s measurements relative to muscle surface area.

Although LD is a valuable tool, it generally relies on few L_s measurements per muscle sample to extrapolate whole muscle properties. Since L_s has rarely been quantified throughout whole muscles (Takahashi et al., 2007), little is known about the degree to which L_s varies at this size scale and impacts muscle function. Interestingly, two-dimensional maps of the TA reveal prominent meso-scale L_s variations (Fig. 2C) whereby systematic L_s differences of about 0.2 µm are observed from the superficial to deep muscle aspects. The anatomical or structural basis for this variation is not clear. This two-dimensional approach is easily generalized to three-dimensional data by measuring L_s from serial sections (Fig. 4). Future work will quantify and model three-dimensional L_s variations and test whether L_s homogeneity is altered in pathological muscle.

Acknowledgements
We are grateful to Shannon Bremner and Mary Esparza for their technical assistance.

Competing interests
The authors declare no competing or financial interests.

Author contributions
S.M.O. and R.L.L. designed the device. S.M.O. programmed the diffraction analysis routine. S.M.O. and E.J.C. collected and processed samples, and analyzed data. The manuscript was composed by S.M.O., with revisions by E.J.C., K.W.Y., S.R.W. and R.L.L.

Funding
This work was supported by the National Institutes of Health [P30 AR058878, R24 HD050837]; and the US Department of Veterans Affairs. Deposited in PMC for release after 12 months.

References
Felder, A., Ward, S. R. and Lieber, R. L. (2005). Sarcomere length measurement permits high resolution normalization of muscle fiber length in architectural studies. *J. Exp. Biol.* **208**, 3275-3279.
Garcia, D. (2010). Robust smoothing of gridded data in one and higher dimensions with missing values. *Comput. Stat. Data Anal.* **54**, 1167-1178.
Gordon, A. M., Huxley, A. F. and Julian, F. J. (1966). The variation in isometric tension with sarcomere length in vertebrate muscle fibres. *J. Physiol.* **184**, 170-192.
Huxley, A. F. and Peachey, L. D. (1961). The maximum length for contraction in vertebrate striated muscle. *J. Physiol.* **156**, 150-165.
Lieber, R. L. (2010). *Skeletal Muscle Structure, Function, and Plasticity: The Physiological Basis of Rehabilitation*. Lippincott Williams & Wilkins.
Lieber, R. L., Yeh, Y. and Baskin, R. J. (1984). Sarcomere length determination using laser diffraction. Effect of beam and fiber diameter. *Biophys. J.* **45**, 1007-1016.
Lieber, R. L., Fazeli, B. M. and Botte, M. J. (1990). Architecture of selected wrist flexor and extensor muscles. *J. Hand Surg. Am.* **15**, 244-250.
Mathieu-Costello, O. (1987). Capillary tortuosity and degree of contraction or extension of skeletal muscles. *Microvasc. Res.* **33**, 98-117.
McNeil, P. L. and Khakee, R. (1992). Disruptions of muscle fiber plasma membranes. Role in exercise-induced damage. *Am. J. Pathol.* **140**, 1097-1109.
Scouten, C., O'Connor, R. and Cunningham, M. (2006). Perfusion fixation of research animals. *Microsc. Today* **14**, 26-33.
Takahashi, M., Ward, S. R. and Lieber, R. L. (2007). Intraoperative single-site sarcomere length measurement accurately reflects whole muscle sarcomere length. *J. Hand Surg.* **32**, 612-617.
Takahashi, M., Ward, S. R., Fridén, J. and Lieber, R. L. (2012). Muscle excursion does not correlate with increased serial sarcomere number after muscle adaptation to stretched tendon transfer. *J. Orthop. Res.* **30**, 1774-1780.
Weiwad, W. K. K., Linke, W. A. and Wussling, M. H. P. (2000). Sarcomere length–tension relationship of rat cardiac myocytes at lengths greater than optimum. *J. Mol. Cell. Cardiol.* **32**, 247-259.
Winters, T. M., Takahashi, M., Lieber, R. L. and Ward, S. R. (2011). Whole muscle length-tension relationships are accurately modeled as scaled sarcomeres in rabbit hindlimb muscles. *J. Biomech.* **44**, 109-115.
Yeh, Y., Baskin, R. J., Lieber, R. L. and Roos, K. P. (1980). Theory of light diffraction by single skeletal muscle fibers. *Biophys. J.* **29**, 509-522.
Young, K. W., Dayanidhi, S. and Lieber, R. L. (2014). Polarization gating enables sarcomere length measurements by laser diffraction in fibrotic muscle. *J. Biomed. Opt.* **19**, 117009.